

EBIC studies of minority electron diffusion length in undoped p-type Gallium Oxide

Leonid Chernyak ^{1, a)}, Seth Lovo ¹, Jian-Sian Li ², Chao-Ching Chiang ², Fan Ren ²,
Stephen J. Pearton ³, Corinne Sartel ⁴, Zeyu Chi ⁴, Yves Dumont ⁴,
Ekaterine Chikoidze ⁴, Alfons Schulte ¹, Arie Ruzin ⁵, and Ulyana Shimanovich ⁶

¹ *Department of Physics, University of Central Florida, Orlando, FL 32816, USA*

² *Department of Chemical Engineering, University of Florida, Gainesville, FL 32611, USA*

³ *Department of Materials Science and Engineering, University of Florida,
Gainesville, FL 32611, USA*

⁴ *Groupe d'Etude de la Matière Condensée, Université Paris-Saclay, Université de Versailles
Saint Quentin en Yvelines – CNRS, 45 Av. des Etats-Unis, 78035 Versailles Cedex, France*

⁵ *School of Electrical Engineering, Tel Aviv University, Tel Aviv 69978, Israel*

⁶ *Department of Molecular Chemistry and Materials Science, Weizmann Institute of Science,
Rehovot 7610001, Israel*

Minority carrier diffusion length in undoped p-type Gallium Oxide was measured at variable temperatures as a function of electron beam charge injection using Electron Beam-Induced Current technique *in-situ* in Scanning Electron Microscope. The results demonstrate that charge injection into p-type β -Gallium Oxide leads to a significant linear increase of minority carrier diffusion length followed by its saturation. The effect was ascribed to trapping of non-equilibrium electrons (generated by a primary electron beam) on meta-stable native defect levels in the material, which in turn blocks recombination through these levels. While the previous studies of the same material were focused on probing a non-equilibrium carrier recombination by purely optical means

This is the author's peer reviewed, accepted manuscript. However, the online version of record will be different from this version once it has been copyedited and typeset.

PLEASE CITE THIS ARTICLE AS DOI: 10.1063/5.0238027

(cathodoluminescence), in this work, the impact of charge injection on minority carrier diffusion was investigated. The activation energy of ~ 0.072 eV, obtained for the phenomenon of interest, is consistent with the involvement of Ga vacancy-related defects.

a) Author to whom correspondence should be addressed: chernyak@physics.ucf.edu

I. Introduction

The minority electron diffusion length in p-type Gallium Oxide is a critical parameter that significantly influences the performance of devices based on this material. Understanding the factors that affect diffusion length and employing appropriate measurement techniques are essential for optimizing the design and fabrication of high-performance Gallium Oxide-based devices [1-6].

Minority electron diffusion length in Gallium Oxide is affected by various factors such as [7]:

1. **Material quality:** The presence of defects, impurities, and crystal imperfections can act as recombination centers, reducing the diffusion length. High-quality gallium oxide with minimal defects is essential for achieving longer diffusion lengths.
2. **Impurity concentration:** The acceptor/donor doping level in gallium oxide affects the concentration of minority carriers. A higher doping concentration can lead to increased recombination, reducing the diffusion length.
3. **Temperature:** In Gallium Oxide, the diffusion length generally decreases with increasing temperature due to enhanced thermal vibrations and increased recombination rates.
4. **Electric field:** The presence of an electric field can influence the diffusion of minority carriers, potentially affecting the diffusion length.

A long minority electron diffusion length is desirable for several reasons [8]:

1. **Efficient charge carrier transport:** Longer diffusion lengths allow minority carriers to travel further before recombining, improving the efficiency of devices such as solar cells and light-emitting diodes.
2. **Reduced recombination losses:** A longer diffusion length reduces the rate of recombination, leading to lower power losses in devices like power transistors.

3. Improved device performance: Devices with longer diffusion lengths generally exhibit better performance characteristics, such as higher efficiency, lower operating voltage, and improved reliability.

During the last several decades, extensive studies were carried out to understand the impact of temperature and doping level on the minority carrier diffusion length in such wide band gap semiconductors as GaN, AlGaIn, and ZnO [9-11]. These studies were complemented by investigation of charge injection impact on minority carrier transport [12-15]. The latter injection results in a several-fold temperature-sensitive increase of diffusion length followed by its saturation. The effect was ascribed to charge trapping on meta-stable native defect levels.

Minority carrier transport studies in Gallium Oxide were first carried out in n-type material, because Ga₂O₃ epitaxial layers are very often grown with electrons being majority carriers [16, 17]. With p-type hetero-epitaxial Gallium Oxide becoming available, minority electron diffusion length was first measured as a function of temperature and charge injection in highly resistive (π -type) material [18]. Very recently, undoped p-type homoepitaxial Ga₂O₃ layers with much higher electrical conductivity were grown and tested by purely optical means (Cathodoluminescence (CL)) *in-situ* in Scanning Electron Microscope under continuous electron beam irradiation (charge injection) [19]. CL intensity decay with increasing duration of electron beam irradiation was ascribed to non-equilibrium electron trapping on Gallium vacancy-related levels in Gallium Oxide forbidden gap, which, in turn, leads to a longer non-equilibrium minority carrier lifetime in the conduction band and consequently to the longer minority electron diffusion length. The activation energy associated with the impact of electron beam irradiation (injection) on CL emission intensity was estimated at ~ 0.3 eV.

In this work, the systematic Electron Beam-Induced Current (EBIC) measurements were performed on (010) Ga₂O₃ homoepitaxial films, as in ref. [19], under variable temperatures and durations of electron beam irradiation to obtain the activation energies for the impact of both parameters (temperature and duration of charge injection) on the minority carrier transport. Another goal was to complement the independent variable temperature CL measurements reported in the ref. [19]. This work is especially relevant given the recent advances in exploiting bipolar transport in NiO/Ga₂O₃ heterojunction rectifiers for power switching applications to overcome limitations in native p-type doping of Ga₂O₃ [20, 21].

II. Experimental

Undoped 1 μm -thick β -Ga₂O₃ was grown on (010)-oriented insulating Fe-doped Ga₂O₃ in a RF-heated horizontal metalorganic chemical vapor deposition (MOCVD) reactor using Ga/O ratio and growth temperature of 1.4×10^{-4} and 775 °C, respectively [22, 23]. X-ray diffraction revealed high quality layer of β -Ga₂O₃ with monoclinic space group ($C2/m$) symmetry.

Metal contacts for electrical characterization were prepared by Ti/Au deposited at the four corners of the sample in a Van der Pauw configuration. The contacts were tested by measuring I-V characteristics, which showed the Ohmic dependence in the temperature range of 450-850 K. Because the contacts exhibited deviation from the linear I-V dependence below 450 K, the Hall effect measurements were not conducted at room temperature. The positive Hall voltage increased with increasing magnetic field, thus confirming the p -type nature of the epitaxial layer with hole concentration $p \sim 2.8 \times 10^{17} \text{ cm}^{-3}$ and resistivity $\rho \sim 0.39 \Omega \cdot \text{cm}$ at 450 K.

Minority carrier diffusion length, L , measurements were carried out using Electron Beam-Induced Current technique *in-situ* in Phillips XL-30 SEM using planar line-scan electron beam

excitation with an electron beam moving along the sample's surface [7, 9, 12, 17, 18]. The EBIC measurements were carried out at room temperature under an electron beam accelerating voltage of 20 kV (to cover the whole epitaxial layer thickness), corresponding to ~ 0.6 nA absorbed current (measured with Keithley 480 picoammeter) and ~ 1 μm electron range (penetration depth) in the material [24]. The EBIC line-scans (16.3 μm lateral length) for diffusion length extraction were carried out using Ni/Au (20 nm/80 nm) asymmetrical pseudo-Schottky contacts created on the film with lithography/lift-off techniques.

A single line-scan takes approximately 12 seconds, which is sufficient for extraction of minority carrier diffusion length value from the exponential decay of Electron Beam-Induced Current in agreement with the following equation [24-26]:

$$I(d) = I_0 d^\alpha \exp\left(-\frac{d}{L}\right) \quad (1)$$

Here, $I(d)$ is the Electron Beam-Induced Current signal as a function of coordinate, d ; I_0 is a scaling factor; d is the coordinate measured from the edge of the contact (Ni/Au) stack; α is a recombination coefficient (set at -0.5).

Fig. 1 shows the initial (nearly zero-injection; no more than 12 seconds) room temperature dependence of the Electron Beam-Induced Current on the distance from the edge of the Schottky barrier. EBIC signal was amplified with Stanford Research Systems SR 570 low-noise current amplifier and digitized with Keithley DMM 2000, controlled by a PC using home-made software.

The inset of Fig. 1 shows the $\ln(I \times d^{1/2})$ dependence on coordinate, d . The minority carrier (electron) diffusion length, L , is extracted as an inverse slope of the linear dependence in the inset of Fig. 1. The value of $L \sim 0.95$ μm was obtained for a nearly-zero injection duration.

To perform electron injection in the region of EBIC measurements, line-scans were not interrupted for the total time of up to ~ 800 seconds (corresponding to the primary excitation electron charge density of $2.1 \times 10^{-7} \text{ C}/\mu\text{m}^3$). The values of diffusion length were periodically extracted using equation (1) for different incremental durations of electron injection varying from nearly zero (for the first line-scan) to 800 seconds. For each measurement temperature, the EBIC dependence as a function of electron beam irradiation duration was measured in a different region in the vicinity of the Schottky barrier under test, to avoid uncontrolled impact of charge injection on minority carrier diffusion length.

It should be noted that the primary excitation SEM electron beam serves for generation of non-equilibrium electron-hole pairs in the material due to the band-to-band (valence band to conduction band) transition of excited electrons. The primary excitation electrons do not accumulate in the material since the sample is grounded, thus preserving the sample's electroneutrality.

III. Results and discussions

The experiments started with variable temperature minority electron diffusion length measurements prior to continuous electron beam irradiation. The results presented in Fig. 2 show a decrease of L with increasing temperature, which is consistent with the previous findings in n-type and highly resistive π -type Ga_2O_3 [16, 18]. Relatively large ($\sim 1 \mu\text{m}$ at room temperature) values of L , obtained in this work, as compared to the n-type samples (several hundred nm) measured in ref. [16], provide an additional proof for material's p-type of conductivity. Within the current temperature range of measurements, it is likely that the origin of L decrease is due to phonon scattering [25].

The temperature dependence of L is represented by the equation (2) [17, 25]:

$$L(T) = L_0 \exp\left(\frac{\Delta E_{A,T}}{2kT}\right) \quad (2)$$

Here, L_0 is a scaling constant; $\Delta E_{A,T}$ is the thermal activation energy; k is the Boltzmann constant; and T is the temperature. The activation energy pertaining to the reduction of L with temperature is estimated at 40 meV. A detailed discussion regarding the origin of $\Delta E_{A,T}$ is presented in ref. [25].

Fig. 3 presents results of the electron injection experiments carried out at variable temperature. Minority electron diffusion length exhibits a linear increase with duration of electron injection before saturation occurs (not shown in Fig. 3). The linear increase of L with electron injection duration was previously observed in p-GaN and p-AlGaN [12-14], p-ZnO [15], unintentionally doped GaN [26], n-Ga₂O₃ [17], and π -Ga₂O₃ [18]. Minority carrier diffusion length increase in Fig. 3 is characterized by the rate R (dL/dt ; where t - is duration of electron injection), which drops from 4 nm/s at 233 K to 0.8 nm/s at 353 K as shown in the inset of Fig. 3.

The effect of temperature on rate R is described by [18]:

$$R(T) = R_0 \exp\left(\frac{\Delta E_{A,T}}{2kT}\right) \exp\left(\frac{\Delta E_{A,I}}{kT}\right) \quad (3)$$

Here R_0 is a scaling constant and $\Delta E_{A,I}$ is the electron injection effect activation energy. Equation (3) can be used to find the activation energy of injection-induced component for the increase in L from the Arrhenius plot in Fig. 4. The slope of the Arrhenius plot is $\Delta E_{A,I} + 0.5\Delta E_{A,T}$, from which $\Delta E_{A,I} \sim 72$ meV is obtained. $\Delta E_{A,I}$ is associated with the mechanism responsible for the elongation of L with injected charge.

Refs. [27, 28] summarize traps in Ga₂O₃, which are associated with native defects and impurities. According to [27], Gallium vacancy (V_{Ga}) – related energetic levels are located at 0.1-0.3 eV and 0.3-0.5 eV above the top of the valence band. In the previous work, focused on electron

beam irradiation impact on minority carrier diffusion length in highly resistive π -type Ga_2O_3 [18], the activation energy around 91 meV was identified. The relatively close values for the activation energies (72 meV, measured in this work, versus 91 meV, reported in ref. [18]) obtained for the different samples with the different majority hole concentrations suggest involvement of the same defect levels in both cases. At the same time, the lower value of $\Delta E_{A,I}$ reported here is likely related to the higher majority hole concentration for the material tested in this investigation.

Ref. [19] reports studies of charge injection-induced effects using Cathodoluminescence technique on the same material as in this work. A non-equilibrium electron, generated by a primary scanning electron microscope beam, gets trapped by deep levels in Ga_2O_3 [18]. Because of a relatively “deep” energetic position in the Ga_2O_3 forbidden gap, a pronounced number of the defects, associated with these deep levels, remains in the neutral state, thus acting as meta-stable electron traps. Trapping non-equilibrium electrons on the defect levels (traps) in the forbidden gap of Gallium Oxide prevents additional recombination of the conduction band electrons through these levels. This leads to an increase of lifetime, τ , for non-equilibrium electrons in the conduction band and, as a result, to an increase of minority carrier diffusion length, L , in agreement with the equation (4) [29]:

$$L = \sqrt{D\tau} \quad (4)$$

(where D is a non-equilibrium carrier diffusion coefficient). Consequently, an increase of τ results in a reduction of radiative recombination events, expressed in a continuous decrease of CL peak intensity with increased duration of electron beam irradiation.

The activation energy of ~ 0.3 eV, associated with the impact of electron beam irradiation (injection) on CL emission intensity as reported in ref. [19], was ascribed to Gallium vacancy-

related point defects [27]. These defects don't necessarily determine the p-type electrical conductivity in the sample but play a significant role in the charge trapping effects. The relative proximity of the activation energies, previously obtained from the CL measurements for the same material, as studied in ref. [19], and the EBIC measurements reported here, suggests similarity of involved defect levels in both cases.

Based on the activation energy of 72 meV, obtained in this work for a Gallium vacancy-related acceptor, its concentration, N_A , could be obtained accounting for Hall majority carrier (hole) concentration ($2.8 \times 10^{17} \text{ cm}^{-3}$ at $T = 450 \text{ K}$). The value of $N_A \sim 1.8 \times 10^{18} \text{ cm}^{-3}$ was obtained from the equation (5) [29].

$$p(T) = N_A \exp\left(-\frac{\Delta E_{A,I}}{kT}\right) \quad (5)$$

It should be finally noted that the recent results in n-type Gallium Oxide provide more information on the possible location of V_{Ga} -related traps [30-32]. In relation to these findings in n-type material, more research is needed in still poorly investigated p-type Gallium Oxide.

IV. Conclusions

Minority electron diffusion length measurements carried out in this work using EBIC technique under variable temperatures and durations of electron beam irradiation revealed a continuous decrease of L with increasing temperature and a continuous elongation of the same parameter with increasing duration of irradiation. Both trends are consistent with the previously published results for highly resistive π -type Ga_2O_3 [18] and indicate involvement of the same Gallium vacancy-related levels in the majority hole conductivity. The lower value of $\Delta E_{A,I}$ reported in this work, as compared to the ref. [18], is likely related to the higher majority hole concentration

for the material tested in this investigation. To conclude, the Gallium vacancy-related acceptor concentration was estimated at $N_A \sim 1.8 \times 10^{18} \text{ cm}^{-3}$.

Acknowledgements

The research at UCF was supported in part by NSF (ECCS2310285; ECCS2341747; ECCS 2427262), US-Israel BSF (award # 2022056) and NATO (awards # G6072; G6194). The work at UF was performed as part of the Interaction of Ionizing Radiation with Matter University Research Alliance (IIRM-URA), sponsored by the Department of the Defense, Defense Threat Reduction Agency under award HDTRA1-20-2-0002, monitored by Jacob Calkins. The present work is a part of "GALLIA" International Research Project, CNRS, France. GEMaC colleagues acknowledge financial support of French National Agency of Research (ANR), project "GOPOWER", CE-50 N0015-01. French and Israeli researchers acknowledge the collaborative PHC-Maimonide project N50047TD. Research at Tel Aviv University was partially supported by the US-Israel BSF (award # 2022056) and NATO (awards # G6072).

Conflict of Interest

The authors have no conflict to disclose.

Data Availability

The data that supports the findings of this study is available within the article.

References

1. S.J. Pearton, J. Yang, P.H. Cary, F. Ren, J. Kim, M.J. Tadjer, and M.A. Mastro, *Appl. Phys. Rev.*, **5**, 011301 (2018).
2. J.Y. Tsao, S. Chowdhury, M.A. Hollis, D. Jena, N.M. Johnson, K.A. Jones, R.J. Kaplar, S. Rajan, C.G. Van de Walle, E. Bellotti, C.L. Chua, R. Collazo, M.E. Coltrin, J.A. Cooper, K.R. Evans, S. Graham, T.A. Grotjohn, E.R. Heller, M. Higashiwaki, M.S. Islam, P.W. Juodawlkis, M.A. Khan, A.D. Koehler, J.H. Leach, U.K. Mishra, R.J. Nemanich, R.C.N. Pilawa-Podgurski, J.B. Shealy, Z. Sitar, M.J. Tadjer, A.F. Witulski, M. Wraback, and J.A. Simmons, *Adv. Electron. Mater.*, **4**, 1600501 (2018).
3. H. von Wenckstern, *Adv. Electron. Mater.*, **3**, 1600350 (2017).
4. M. Kim, J.-H. Seo, U. Singiseti, and Z. Ma, *J. Mater. Chem.*, **C 5**, 8338 (2017).
5. M. Higashiwaki, K. Sasaki, H. Murakami, Y. Kumagai, A. Koukitu, A. Kuramata, T. Masui, and S. Yamakoshi, *Semicond. Sci. Technol.*, **31**, 034001 (2016).
6. A. Kuramata, K. Kimiyoshi, W. Shinya, Y. Yu, M. Takekazu, and Y. Shigenobu, *Jpn. J. Appl. Phys.*, Part 1, **55**, 1202A2 (2016).
7. S. Modak, A. Ruzin, A. Schulte, and L. Chernyak, *Condens. Matter*, **9**, 2 (2024).
8. L. Chernyak, A. Osinsky, and A. Schulte, *Solid-State Electronics*, **45**, 1687 (2001).
9. L. Chernyak, A. Osinsky, H. Temkin, J.W. Yang, Q. Chen, and M. Asif Khan, *Appl. Phys. Lett.*, **69**, 2531 (1996).
10. W. Burdett, A. Osinsky, V. Kotlyarov, P. Chow, A. Dabiran, L. Chernyak, *Solid-State Electron.*, **47**, 931 (2003).
11. O. Lopatiuk-Tirpak, L. Chernyak, *Superlattices and Microstructures*, **42**, 201 (2007).

12. Leonid Chernyak, Andrei Osinsky, Vladimir Fuflyigin, E.F. Schubert, *Appl. Phys. Lett.*, **77**, 875 (2000).
13. W. Burdett, A. Osinsky, V. Kotlyarov, P. Chow, A. Dabiran, L. Chernyak, *Solid-State Electron.*, **47**, 931 (2003).
14. O. Lopatiuk, A. Osinsky, A. Dabiran, K. Gartsman, I. Feldman, L. Chernyak, *Solid-State Electron.*, **49**, 1662 (2005).
15. O. Lopatiuk-Tirpak, L. Chernyak, F.X. Xiu, J.L. Liu, S. Jang, F. Ren, S.J. Pearton, K. Gartsman, Y. Feldman, A. Osinsky, P. Chow, *J. Appl. Phys.*, **100**, 086101 (2006).
16. J. Lee, E. Flitsiyan, L. Chernyak, J.C. Yang, F. Ren, S. Pearton, B. Meyler, Y.J. Salzman, *Appl. Phys. Lett.*, **112**, 082104 (2018).
17. S. Modak, J. Lee, L. Chernyak, J. Yang, F. Ren, S. J. Pearton, S. Khodorov, and I. Lubomirsky, *AIP Adv.*, **9**, 015127 (2019).
18. Sushrut Modak, Alfons Schulte, Corinne Sartel, Vincent Sallet, Yves Dumont, Ekaterine Chikoidze, Xinyi Xia, Fan Ren, Stephen J. Pearton, Arie Ruzin, and Leonid Chernyak, *Appl. Phys. Lett.*, **120**, 233503 (2022).
19. Leonid Chernyak, Alfons Schulte, Jian-Sian Li, Chao-Ching Chiang, Fan Ren, Stephen J. Pearton, Corinne Sartel, Vincent Sallet, Zeyu Chi, Yves Dumont, Ekaterine Chikoidze, and Arie Ruzin, *AIP Adv.*, **14**, 085103 (2024).
20. F. Zhou, H. Gong, M. Xiao, Yunwei Ma, Zhengpeng Wang Xinxin Yu, Li Li, Lan Fu, Hark Hoe Tan, Yi Yang, Fang-Fang Ren, Shulin Gu, Youdou Zheng, Hai Lu, Rong Zhang, Yuhao Zhang and Jiandong Ye, *Nat Commun* **14**, 4459 (2023).

21. Jian-Sian Li, Hsiao-Hsuan Wan, Chao-Ching Chiang, Timothy Jinsoo Yoo, Meng-Hsun Yu, Fan Ren, Honggyu Kim, Yu-Te Lia and Stephen J. Pearton, *ECS J. Solid State Sci. Technol.*, **13**, 035003 (2024).
22. Z. Chi, J.J. Asher, M.R. Jennings, E. Chikoidze, A. Pérez-Tomás, *Materials*, **15**, 1164 (2022).
23. Z. Chi, C. Sartel, Y. Zheng, S. Modak, L. Chernyak, C.M. Schaefer, J. Padilla, J. Santiso, A. Ruzin, A.M. Gonçalves, J. von Bardeleben, G. Guillot, Y. Dumont, A. Pérez-Tomás, E. Chikoidze, *Journal of Alloys and Compounds*, **969**, 172454 (2023).
24. E.B. Yakimov, A.Y. Polyakov, I.V. Shchemerov, N. B. Smirnov, A.A. Vasilev, P.S. Vergeles, E.E. Yakimov, A.V. Chernykh, F. Ren and S.J. Pearton, *Appl. Phys. Lett.*, 118, 202106 (2021).
25. S. Modak, L. Chernyak, A. Schulte, C. Sartel, V. Sallet, Y. Dumont, E. Chikoidze, X. Xia, F. Ren, S.J. Pearton, A. Ruzin, D.M. Zhigunov, S.S. Kosolobov, and V.P. Drachev, *APL Mater.*, **10**, 031106 (2022).
26. S. Modak, L. Chernyak, M.H. Xian, F. Ren, S.J. Pearton, S. Khodorov, I. Lubomirsky, A. Ruzin, and Z. Dashevsky, *J. Appl. Phys.*, **128**, 085702 (2020).
27. M. Labeled, N. Sengouga, C.V. Prasad, M. Henini, *Materials Today Physics*, **36**, 101155 (2023).
28. A.Y. Polyakov, N.B. Smirnov, I.V. Shchemerov, S.J. Pearton, F. Ren, A.V. Chernykh, P.B. Lagov, T.V. Kulevoy, *APL Mater.*, **6**, 096102 (2018).
29. S.M. Sze, *Physics of Semiconductor Devices*, J. Wiley & Sons, New York (1969).
30. F. Tuomisto, *Jap. J. Appl. Phys.*, **62**, SF0802 (2023).
31. I. Zhelezova, I. Makkonen, F. Tuomisto, *J. Appl. Phys.*, **136**, 065702(2024).
32. Amanda Langørgen, Lasse Vines, Ymir Kalmann Frodason, *J. Appl. Phys.* 135, 195702 (2024).

Figure Captions

Fig. 1. Room temperature initial (nearly zero injection duration) EBIC signal decay as function of distance from the edge of the Schottky contact. Line-scan duration is 12 seconds.

Inset: Extraction of minority electron diffusion length, L , according to the equation (1). L value obtained from the inverse slope of the linear fit is $0.95 \mu\text{m}$.

Fig. 2. Dependence of the initial (nearly zero injection) L values on temperature and the exponential fit according to the equation (2). Different locations on the sample's surface were selected for each measurement temperature.

Inset: Extraction of the activation energy $\Delta E_{A,T}$ (40 meV) from the Arrhenius plot for L versus T dependence according to the equation (2). The activation energy is obtained as a slope of the linear fit.

Fig. 3. Impact of electron beam irradiation duration on minority electron diffusion length at various temperatures and the respective linear fits. The rate R at each temperature is obtained as the slope of the linear fit.

Inset: R dependence for each measurement temperature and the exponential fit according to the equation (3).

Fig. 4. Arrhenius plot for the rate R as a function of temperature. The activation energy of 72 meV is obtained as a slope of the linear fit.

This is the author's peer reviewed, accepted manuscript. However, the online version of record will be different from this version once it has been copyedited and typeset.
PLEASE CITE THIS ARTICLE AS DOI: 10.1063/1.50238027

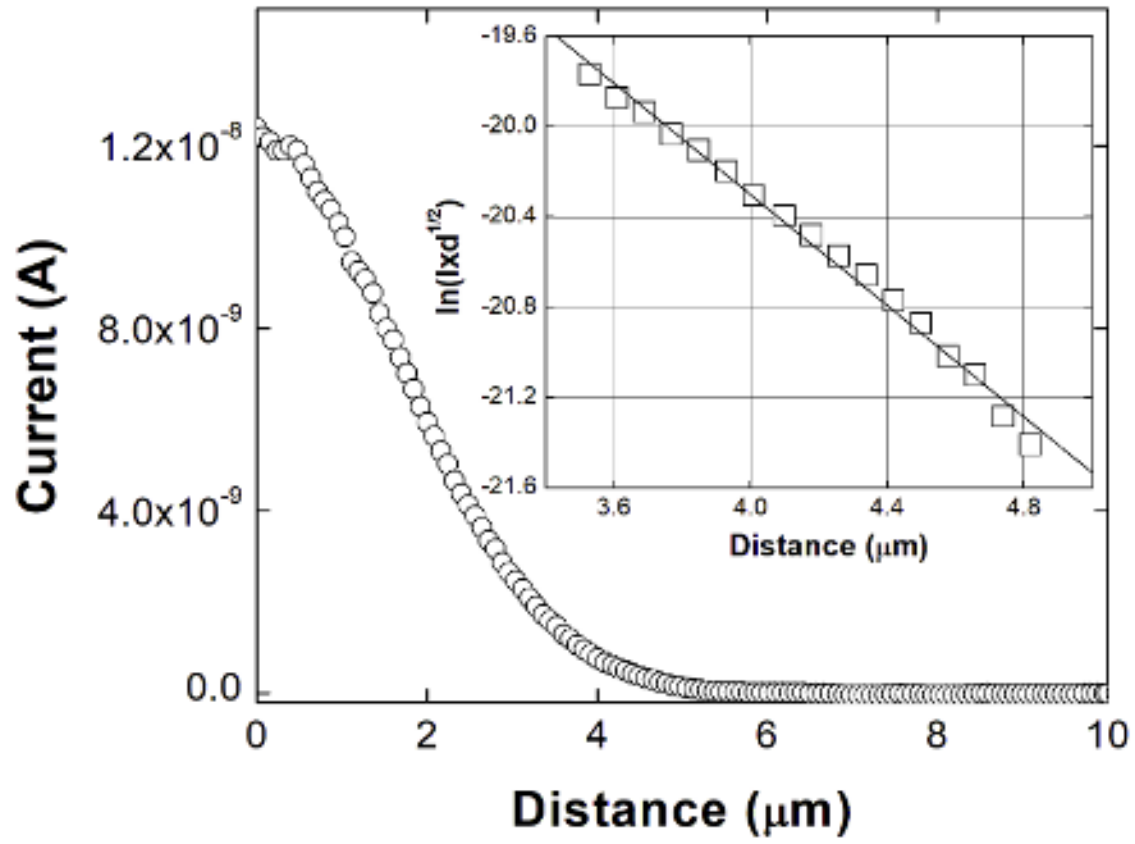


Fig. 1

This is the author's peer reviewed, accepted manuscript. However, the online version of record will be different from this version once it has been copyedited and typeset.
PLEASE CITE THIS ARTICLE AS DOI: 10.1063/1.50238027

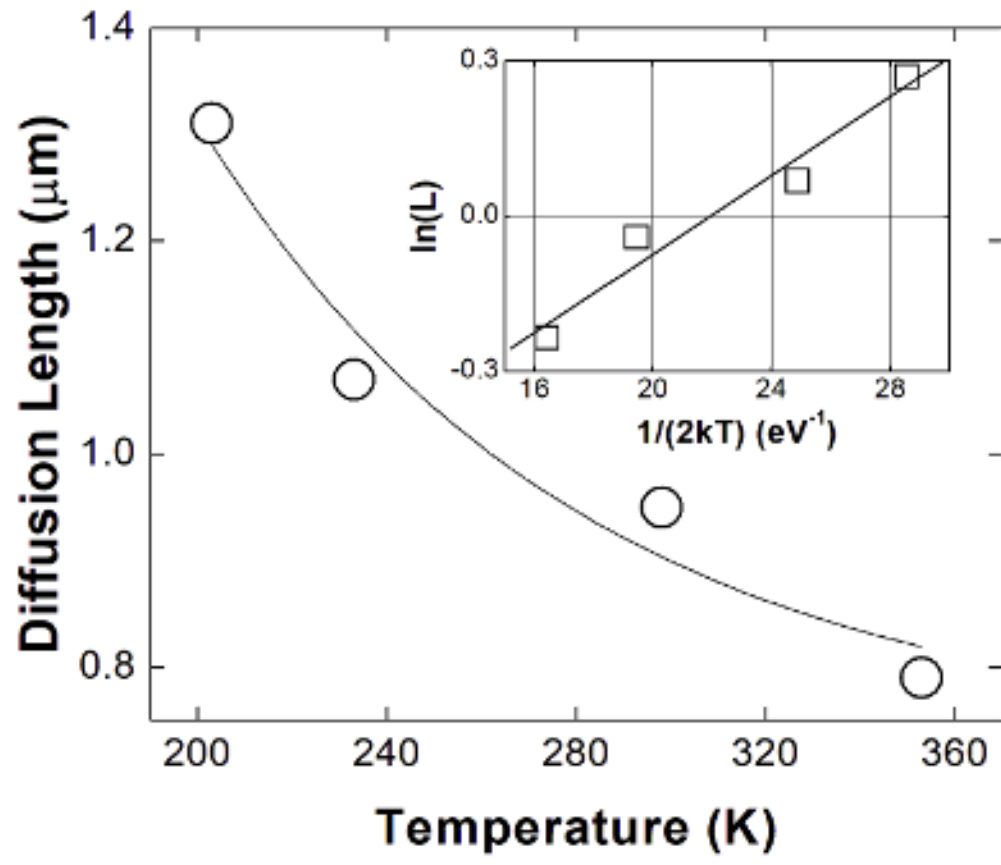
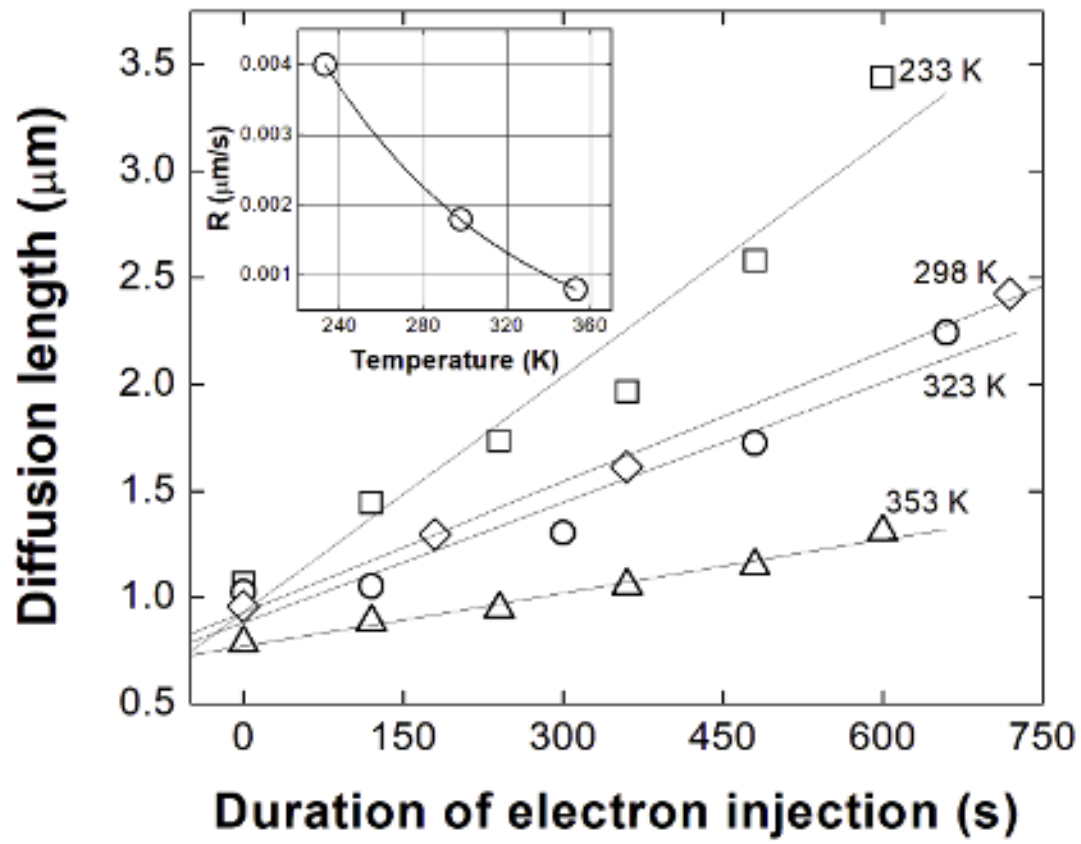


Fig. 2

This is the author's peer reviewed, accepted manuscript. However, the online version of record will be different from this version once it has been copyedited and typeset.
PLEASE CITE THIS ARTICLE AS DOI: 10.1063/1.5238027

Fig. 3



This is the author's peer reviewed, accepted manuscript. However, the online version of record will be different from this version once it has been copyedited and typeset.
PLEASE CITE THIS ARTICLE AS DOI: 10.1063/1.50238027

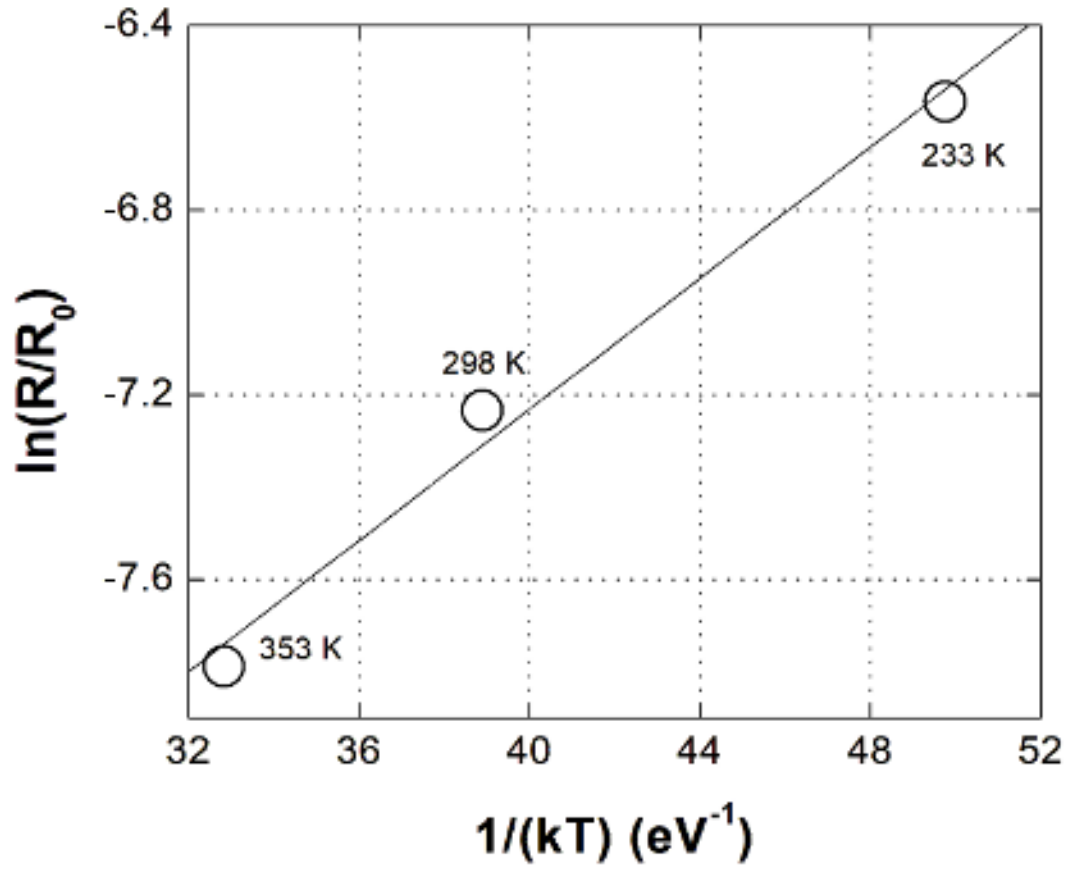


Fig. 4